RF-sputtered HfO_2 Gate Insulator in High-Performance AlGaN/GaN MOS-HEMTs

Ogyun Seok[a], Woojin Ahn[a], Min-Woo Ha[b], and Min-Koo Han[a]

[a] Department of Electrical Engineering and Computer Science, Seoul National University,
Seoul 151-744, Korea
[b] Korea Electronics Technology Institute, Seongnam, Gyeongi-do 463-816, Korea

We have proposed and fabricated AlGaN/GaN metal-oxide-semiconductor-high-electron-mobility transistors (MOS-HEMTs) on Si substrate employing RF-sputtered HfO_2 gate insulator for a high breakdown voltage. The HfO_2 sputtering conditions such as a sputtering power and working pressure have been optimized in order to improve reverse blocking characteristics. We obtained the high breakdown voltage of 1524 V, the low drain leakage current of 67 pA/mm when V_{DS}= 100 V and V_{GS}= –10 V, and on/off current ratio of 2.37×10^{10} at sputtering power of 50 W and working pressure of 3 mTorr. In addition, we also discussed the mechanism of breakdown voltage improvement and investigated HfO_2/GaN interface in the proposed devices by measuring the leakage current, capacitance-voltage characteristics, and X-ray diffraction (XRD).

Introduction

AlGaN/GaN high-electron-mobility transistors (HEMTs) have received a considerable attention for high-power applications due to their wide bandgap properties, such as high critical electric field, low intrinsic carrier concentration, and high velocity saturation [1]. In addition, piezoelectric polarization, which are unique characteristics in AlGaN/GaN heterostructures, offers high-mobility and high-density two dimensional electron gas so that AlGaN/GaN HEMTs are also suitable for high-speed and high-current applications [2].

However, surface leakage current caused by an electron trapping from the gate into the shallow states and gate leakage current by trap-assisted tunneling in the Schottky/GaN interface are serious problems to obtain high breakdown voltage in the AlGaN/GaN HEMTs [3]. Metal-oxide-semiconductor (MOS) structure is suitable for blocking of gate leakage current and suppression of surface leakage current. Recently, various gate insulator materials such as SiN_x [4], SiO_2 [5], and Al_2O_3 [6] in the AlGaN/GaN MOS-HEMTs have been reported. We have already reported the high breakdown voltage and the low leakage current by using RF-sputtered HfO_2 gate insulator in the AlGaN/GaN MOS-HEMTs [7]. RF-sputtered HfO_2 has various advantages such as high-*k* characteristics, low cost, high throughput, and low process temperature.

In this paper, we optimized the HfO_2 sputtering conditions in the AlGaN/GaN MOS-HEMTs. The sputtering conditions such as temperature, power, and working pressure have strong dependency on crystallization and blocking characteristics of HfO_2 gate insulator. We sputtered HfO_2 gate insulator on the AlGaN/GaN heterostructure at the various conditions considering crystallization, sputtering damage to GaN surface, and suppression of surface leakage current.

Device Structure and Fabrication

The AlGaN/GaN heterostructure was grown on a Si (111) substrate by metal-organic chemical vapor deposition. The structure includes the following specific layers: a 3.9 µm-thick C-doped GaN buffer layer, a 100 nm-thick i-GaN layer, a 20 nm-thick i-$Al_{0.23}Ga_{0.77}N$ barrier layer, and a 3 nm-thick i-GaN cap layer.

A cross-sectional view of the AlGaN/GaN MOS-HEMTs with HfO_2 gate insulator is shown in Fig. 1. Mesa isolation was carried out to define active regions using Cl_2-based inductively coupled plasma-reactive ion etcher. Ohmic metals of Ti/Al/Ni/Au (20/80/20/100 nm) for the source and the drain formed by e-gun evaporator and lift-off. We annealed the ohmic metals at 880 °C for 40 s. Prior to HfO_2 sputtering, we dipped the devices into 30:1 buffered oxide etchant for 30 s in order to remove a native oxide. 15 nm-thick HfO_2 was deposited by RF-sputtering on the GaN cap layer at the sputtering powers from 50 to 300 W. This was done at room temperature under an Ar flow of 15 sccm. We used working process pressures of 3 and 10 mTorr. The 15 nm-thick HfO_2 was confirmed by scanning electron microscope image as shown in Fig. 2. The HfO_2 gate insulator using RF-sputter showed a linear sputtering-rate against sputtering power and working pressure so that we did sputtering 15 nm-thick HfO_2 gate insulator at the various sputtering powers and working pressure by adjusting the sputtering time. Finally, the Schottky contact, Ni/Au (30/150 nm), was formed on the HfO_2 layer. The gate length, gate-source distance, gate-drain distance, and gate width were 3, 3, 20, and 50 µm, respectively. The conventional AlGaN/GaN HEMT without any gate insulator was also fabricated for comparison purpose.

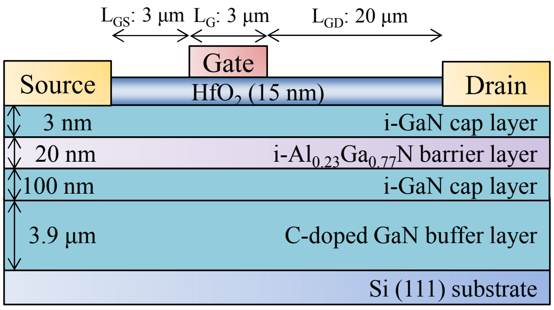

Fig. 1: Cross-sectional view of the AlGaN/GaN MOS-HEMT employing HfO_2 gate insulator

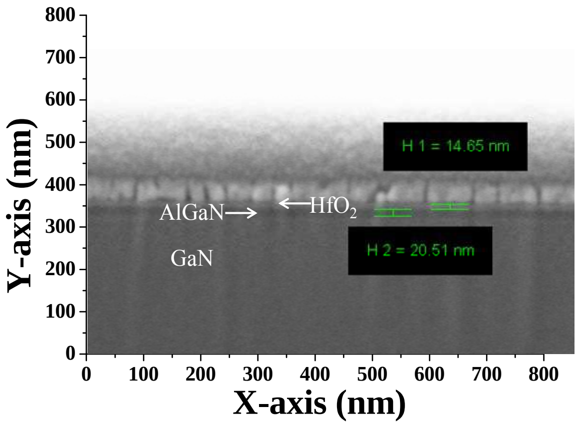

Fig. 2: SEM image of HfO_2/AlGaN/GaN heterostructure

Experimental Results and Discussion

Figure 3 shows the drain leakage currents of the AlGaN/GaN HEMT and MOS-HEMTs with HfO_2 gate insulator sputtered at 50, 150, and 300 W with the fixed working pressure of 3 mTorr. These were measured at V_{GS} of –10 V. The drain current of the conventional HEMT at V_{DS} of 100 V is 192 μA/mm while that of MOS-HEMT with HfO_2 sputtered at 50 W is 67 pA/mm. This suppression of drain leakage current results from the effective blocking characteristics of HfO_2 gate insulator and passivating GaN surface. However, the drain leakage current increases when HfO_2 is sputtered at a high power due to sputtering damage to GaN surface [8]. The AlGaN/GaN MOS-HEMTs with HfO_2 gate insulator sputtered at 150 and 300 W show 18 and 991 nA/mm, respectively.

Figure 4 shows the drain leakage currents of the AlGaN/GaN HEMT and MOS-HEMTs with HfO_2 sputtered at 3 and 10 mTorr with the fixed sputtering power of 50 W. The device with HfO_2 sputtered at 10 mTorr shows the drain leakage current of 2.99 nA/mm. It means that working pressures during HfO_2 sputtering influences on the blocking characteristics of HfO_2 in the AlGaN/GaN MOS-HEMTs.

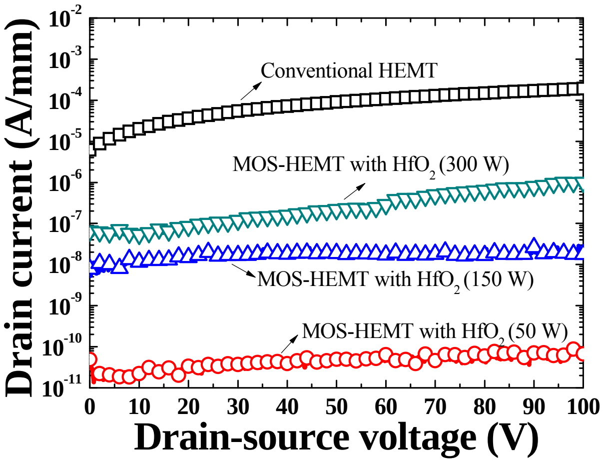

Fig. 3: Drain leakage current of the AlGaN/GaN HEMT and MOS-HEMTs with HfO_2 sputtered at various powers

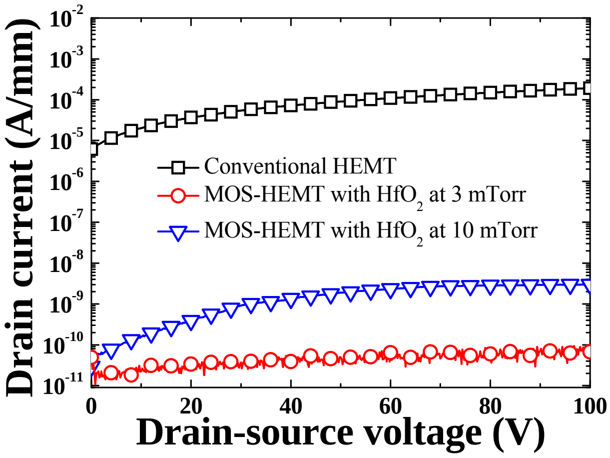

Fig. 4: Drain leakage current of the AlGaN/GaN HEMT and MOS-HEMTs with HfO_2 sputtered at 3 and 10 mTorr

Figure 5 shows the breakdown characteristics of the AlGaN/GaN HEMT and the MOS-HEMTs with HfO_2 gate insulator sputtered at 3 and 10 mTorr with the fixed sputtering power of 50 W. The breakdown voltage was determined at the gate-source voltage of –10 V and the drain leakage current of 1 mA/mm. We obtained the high breakdown voltage of 1524 for the AlGaN/GaN MOS-HEMT with HfO_2 gate insulator sputtered at 3 mTorr while those of the conventional HEMT and MOS-HEMT at 10 mTorr are 470 and 1220 V, respectively. The breakdown voltage of the AlGaN/GaN HEMTs is determined by electron runaway on the surface [9]. The injected electrons into the surface states cause the surface leakage current. Sputtered HfO_2 at 3 mTorr is effective to obtain the low leakage current and the high breakdown voltage compared to 10 mTorr.

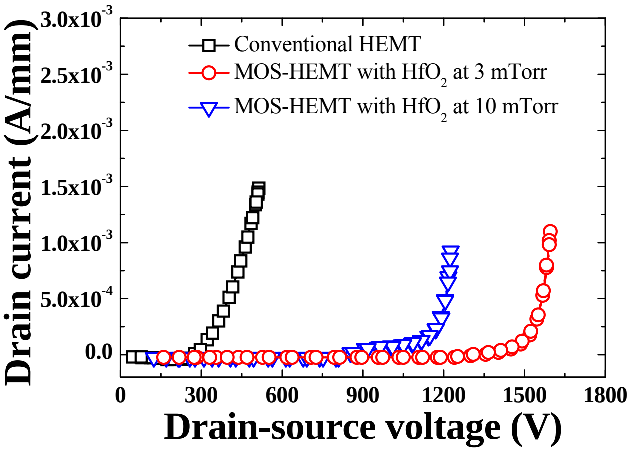

Fig. 5: Breakdown characteristics

We measured the XRD of the sputtered HfO_2 as shown in Fig. 6. HfO_2 was sputtered at 3 and 10 mTorr on p-type Si substrate. The HfO_2 at 3 mTorr shows weak peaks of the (2 0 0) and (2 2 0) tetragonal phases at around 35° [10]. This indicates that the low-process pressure during the HfO_2 sputtering leads to the crystallization of HfO_2. The weakly crystallized HfO_2 at 3 mTorr shows improved dielectric blocking characteristics as shown in Fig. 4 so that HfO_2 gate insulator sputtered at a low working pressure is suitable to AlGaN/GaN MOS-HEMTs compared to a high condition.

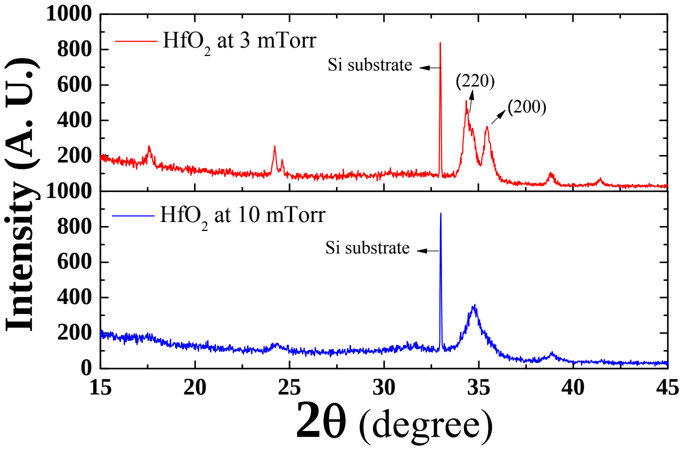

Fig. 6: XRD spectra of the HfO_2 sputtered at 3 and 10 mTorr

Figure 7 shows capacitance-voltage characteristics of the AlGaN/GaN MOS-HEMTs with HfO_2 gate insulator sputtered at 3 mTorr and 50 W. We varied maximum gate-source bias with fixed frequency of 1 MHz to investigate response of electrons to HfO_2/GaN interface states. The curve with sweeping ragnge from –10 to –0.5 V has a small hysteresis of 100 mV near threshold voltage. However, the curve with sweeping range from –10 to 5 V has a large hysteresis of 1.1 V correspoing which results from acceptor-like traps at the HfO_2/GaN interface [11]. The electrons are accumulated at AlGaN barrier layer and capacitance increases with steep slope when gate bias is higher than 2.5 V.

Figure. 8 shows the capacitance-voltage characteristics with measuring frequency of 1, 10, 100 kHz, and 1 MHz. At all frequency conditions, nearly indentical hystesis at the negative gate bias is observed. However, the lower frequency causes the high-capacitance value and the large hysteresis at the positive gate bias. This high-capacitance values are originated from the electron capturing at the oxide/GaN interface [12]. Our results indicate that the electron capturing at HfO_2/GaN interface states is a slow process which responds to the lower frequency than 1 MHz. The most electrons which are captured interface states are emitted at the reverse sweep so that AlGaN/GaN MOS-HEMT with RF-sputtered HfO_2 has stable V_{TH} characteristics at the various operating frequency.

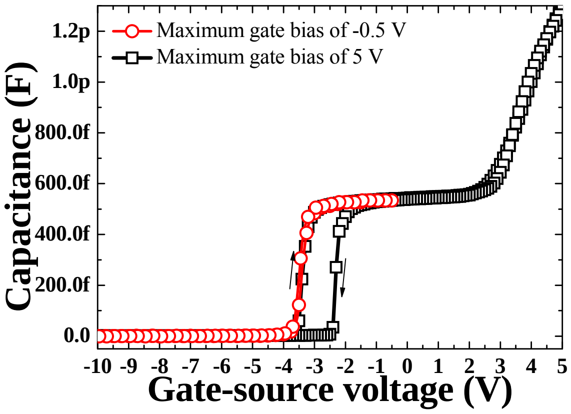

Fig. 7: Capacitance-voltage characteristics of the AlGaN/GaN MOS-HEMTs

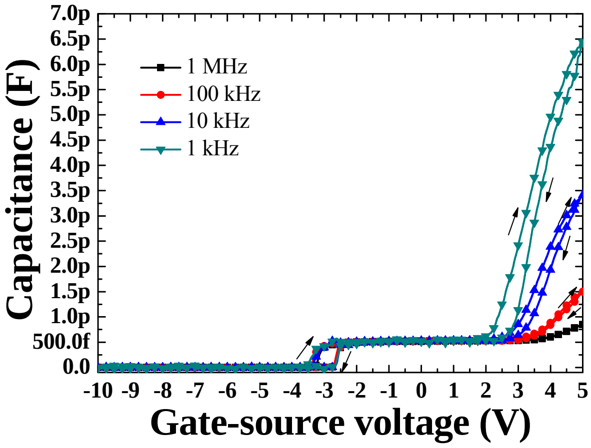

Fig. 8: Capacitance-voltage characteristics of the AlGaN/GaN MOS-HEMTs with various measuring frequency

Conclusion

We optimized the HfO_2 sputtering conditions for high-performance AlGaN/GaN MOS-HEMTs. We onbtained the high breakdown voltage of 1524 V at working pressure of 3 mTorr and sputtering power of 50 W. A low sputtering power improved the reverse blocking characteristics of the AlGaN/GaN MOS-HEMTs due to suppression of sputtering damage to GaN surface. Also, weak crystallization was obersed at the low working pressure. This crystallizatino may contributed to the improved dielectric leakage blocking characteristics, drain leakage current, and breakdown voltage. Finally, we evaluated the interface characteristics of the AlGaN/GaN MOS-HEMT with HfO_2 sputtered at the optimum condition. RF-sputtered HfO_2 gate insulator may be promising in the high-voltage AlGaN/GaN MOS-HEMTs

Acknowledgments

This work was supported by the “Power Generation and Electricity Delivery” of the Korea Institute of Energy Technology Evaluation and Planning (KETEP) grant funded by the Korea Government Ministry of Knowledge Economy. (Project No. 101030002B)

References

1. T. Nomura, H. Kambayashi, M. Masuda, S. Ishii, N. Ikeda, J. Lee, and S. Yoshida, *Proc. Int. Symp. Power Semiconductor Device and ICs*, pp 313, 2006.
2. O. Ambacher, J. Smart, J. R. Shealy, N. G. Weimann, K. Chu, M. Murphy, W. J. Schaff, L. F. Eastman, R. Dimitrov, L. Wittmer, M. Stutzman, W. Rieger, and J. Hilsenbec, *J. Appl. Phys*., **85**(6), 3222 (1999).
3. W. S. Tan, P. A. Houston, P. J. Parbrook, D. A. Wood, G. Hill, C. R. Whitehouse, *Appl. Phys. Lett*., **80**(17), 3207 (2002).
4. V. Adivarahan, J. Yang, A. Koudymov, G. Simin, and M. A. Khan, *IEEE Electron Device Lett*., **26**(8), 535 (2005).
5. M. Kanamura, T. Kikkawa, T. Iwai, K. Imanishi, T. Kubo, and K. Joshin, *Dig. Int. Electron Devices Meet*., pp 572, 2005.
6. M. Kanamura, T. Ohki, T. Kikkawa, K. Imanishi, T. Imada, A. Yamada, and N. Hara, *IEEE Electron Device Lett*., **31**(3), 189 (2010).
7. O. Seok, W. Ahn, M. -K. Han, and M. –W. Ha, *Semicon. Sci, Technol*., **28**(2), 025001 (2013).
8. L. Pang and K. Kim, *J. Phys. D: Appl. Phys*., **45**(4), 0445105 (2012).
9. Z. H. Liu, G. I. Ng, H. Zhou, S. Arulkumaran, and Y. K. T. Maung 2011 *Appl. Phys. Lett*., **98**(16), 113506 (2011).
10. W. S. Tan, P. A. Houston, P. J. Parbrook, D. A. Wood, G. Hil, and C. R. Whitehouse, *Appl. Phys. Lett*., **80**(17) 3207 (2002).
11. C. Mizue, Y. Hori, M. Miczek, and T. Hashizume, *Jpn. J. Appl. Phys*., **50**, 021001 (2011).
12. S. Huang, S. Yang, J. Roberts and K. J. Chen, *Jpn. J. Appl. Phys*., **50**, 110202 (2011).